

## ACCEPTED VERSION

Watts, Michael John; Li, Yuxiao; Russell, Bayden D.; Mellin, Camille; Connell, Sean  
Duncan; Fordham, Damien Anthony

[A novel method for mapping reefs and subtidal rocky habitats using artificial neural networks](#), Ecological Modelling, 2011; 222(15):2606-2614.

Copyright © 2011 Elsevier B.V.

### PERMISSIONS

<http://www.elsevier.com/wps/find/authorsview.authors/rights>

[The author retains] the right to post a revised personal version of the text of the final journal article (to reflect changes made in the peer review process) on your personal or institutional website or server for scholarly purposes, incorporating the complete citation and with a link to the Digital Object Identifier (DOI) of the article.

27<sup>th</sup> August, 2012

<http://hdl.handle.net/2440/67121>

1 | **Published in: *Ecological Modelling*, 2011; 222(15):2606-2614**

2

3

4 | **A novel method for mapping reefs and**  
5 | **subtidal rocky habitats using artificial**  
6 | **neural networks**

---

7

8 | Michael J. Watts<sup>1\*</sup>, Yuxiao Li<sup>1,2</sup>, Bayden Russell<sup>2</sup>, Camille Mellin<sup>1,3</sup>, Sean D.  
9 | Connell<sup>2</sup>, and Damien A. Fordham<sup>1</sup>

10 | <sup>1</sup>The Environment Institute and School of Earth & Environmental Sciences, University of

11 | Adelaide, South Australia 5005, Australia

12 | <sup>2</sup>Southern Seas Ecology Laboratories, School of Earth & Environmental Sciences, University  
13 | of Adelaide, South Australia 5005, Australia

14 | <sup>3</sup>Australian Institute of Marine Science, PMB No.3, Townsville MC, Townsville, Queensland  
15 | 4810, Australia

16

17 | \*corresponding author, e: [mjwatts@ieee.org](mailto:mjwatts@ieee.org)

18

19 **Abstract**

20  
21 Reefs and subtidal rocky habitats are sites of high biodiversity and productivity which  
22 harbour commercially important fish and invertebrate species. Although the  
23 conservation management of reef associated species has been informed using species  
24 distribution models (SDM) and community based approaches, to date their use has  
25 been constrained to specific regions where the locality and spatial extent of reefs is  
26 well known. Much of the world's subtidal habitats remain either undiscovered or  
27 unmapped, including coasts of intense human use. Consequently, to facilitate a  
28 stronger understanding of species-environmental relationships there is an urgent need  
29 for a cost and time effective standard method to map reefs at fine spatial resolutions  
30 across broad geographical extents. We used bathymetric data (~ 250 m resolution) to  
31 calculate the local slope and curvature of the seabed. We then constructed artificial  
32 neural networks (ANNs) to forecast the probability of reef occurrence within grid  
33 cells as a function of bathymetric and slope variables. Testing over an independent  
34 data set not used in training showed that ANNs were able to accurately predict the  
35 location of reefs for 86% of all grid cells (Kappa = 0.63) without over fitting. The  
36 ANN with greatest support, combining bathymetric values of the target grid cell with  
37 the slope of adjacent grid cells, was used to map inshore reef locations around the  
38 Southern Australian coastline (~ 250 m resolution). Broadly, our results show that  
39 reefs are identifiable from coarse-scale bathymetry data of the seabed. We expect that  
40 our research technique will strengthen systematic conservation planning tools in many  
41 regions of the world, by enabling identification of rocky substrate and mapping in  
42 localities that remain poorly surveyed due to logistics or monetary constraints.

43

## 44 **Introduction**

45  
46 Some of the most diverse marine ecosystems are founded on subtidal rock or corals  
47 that fringe the world's coasts or occur as isolated reefs. Such subtidal habitats are  
48 generally known as 'subtidal rocky habitats', 'rocky reefs' or simply 'reefs' (hereafter  
49 referred to as reefs). Identifying the presence and extent of reefs is fundamental if we  
50 are to quantify their contribution to biological and socio-economic productivity  
51 through fisheries production, biological diversity and economic value in marine  
52 ecosystems (Connell and Gillanders, 2007).

53  
54 Species distribution models (SDM; see review by Guisan and Thuiller (2002)) have  
55 been used to predict the distribution of some marine and reef biota (Robinson et al.,  
56 2010), informing conservation management (Mellin et al., 2010a). These models have  
57 for example investigated the environmental and spatial predictors of the diversity and  
58 abundance of coral reef fish (Mellin et al., 2010a); and have been used to map habitat  
59 suitability and range extents of marine invertebrates living in reef environments, for  
60 example, Galparsoro (2009).

61  
62 Unfortunately, the use of SDMs for mapping the habitat suitability and range extent of  
63 reef species, and marine species in general, is often limited by a dearth of spatial data,  
64 including the location of suitable habitat. While fine-scale, remotely sensed maps of  
65 reef distributions are readily available for iconic and well-studied regions (e.g. Great  
66 Barrier Reef, Australia; U.S. Virgin Islands), in most parts of the world the location  
67 and extent of reefs is unknown, and therefore, the fundamental basis for considering  
68 their biological and economic importance is missing. Whilst the acoustic

69 classification of habitats provides information to scales of 0.1 m (Cochrane and  
70 Lafferty, 2002), the cost and time involved in acquiring such information with side-  
71 scan sonar across large tracts of coast (e.g. > 2000 kilometres of coast in Southern  
72 Australia) hampers even the most basic exploration for such habitats. We developed a  
73 method based on artificial neural networks (ANNs) that used coarse-scale bathymetric  
74 data to predict the location and extent of reefs off the southern coast of Australia.

75

76 Artificial neural networks (ANNs) are a useful technique for modelling problems that  
77 involve complex but unknown processes (Crick, 1989; Haykin, 1994; Reed and  
78 Marks, 1999; Tarassenko, 1998). They have many advantages over statistically based  
79 techniques (Kasabov, 1996) because they can learn from existing data and therefore  
80 do not require an *a priori* model. If over fitting is avoided ANN can also generalise  
81 well, in other words, they can accurately classify data they have not been trained on.  
82 Additionally, ANNs can learn from noisy data (Kasabov, 1996) and model systems  
83 that involve multiple dependent variables and complex non-linear relationships  
84 between variables and outcomes. In ecological studies where ANNs have been  
85 compared to traditional statistical models, the ANNs have consistently out-performed  
86 the statistical models with respect to prediction accuracy (Brosse et al., 1999a; Ibarra  
87 et al., 2003; Jeong et al., 2006; Laë et al., 1999; Lek et al., 1996; Manel et al., 1999;  
88 Mastrorillo et al., 1997; Soltic et al., 2004; Wagner et al., 2000; Wagner et al., 2006).

89

90 While ANNs have been previously applied to classifying reefs from video images  
91 (Marcos et al., 2005) and classifying sediments on the seafloor (Zhou and Chen,  
92 2005), we hereby provide the first evidence that ANNs can be used to identify the  
93 presence of reefs from coarse-scale bathymetric data. As a first attempt at addressing

94 this problem with ANN, the goal of this paper was not to exhaustively test the myriad  
95 ANN architectures and training algorithms available (Reed and Marks, 1999) to get  
96 the absolute best model possible. Rather, the goal was to determine whether ANN are  
97 applicable to the generic problem of detecting reefs.

98

99 We were able to create a model of sufficient accuracy to provide the basis for  
100 modelling the spatial abundance patterns of two commercially significant Abalone  
101 species (*Haliotis rubra* and *H. laevigata*) inhabiting inshore rocky reefs of Southern  
102 Australia (Mellin et al., 2010b).

103

## 104 Method

105

### 106 Data

107 We present a map of the study area, from which we sourced the data for this study, in  
108 Figure 1. Two sets of data were combined for this study: (1) bathymetric  
109 measurements at a 250 m resolution, with a depth precision of six metres (Geoscience  
110 Australia, 2009); (2) point sample data that specified the location of observed reefs  
111 around South Australia at a bathymetric depth of less than 30 m. These sample points  
112 were acquired by visual surveys. There were 121 sample points that corresponded to  
113 reefs and 56 sample points that corresponded to non-reef seafloor. Also included were  
114 297 randomly selected points that were known to be on land: the purpose of these  
115 samples were so that the ANNs could learn to distinguish between reefs that reached  
116 or breached the waterline and on-land features that were present in the on-land coastal  
117 buffer region. A second set of sample points (n=317, presence=126, absence=191),  
118 from a different survey, was the validation data set, or independent test set which used  
119 to test the generalisation accuracy of the ANNs. 147 points were randomly removed

120 from the on-land data set and added to the validation data set, as this data set did not  
121 include any on-land survey points. Two of the sample points in the training set were  
122 unusable, as they appeared in the same cells as other sample points and therefore were  
123 redundant. There were thus a total of 325 vectors in the training set and 464 vectors in  
124 the validation set. Additional out-of-area validation data, that is, data from a region  
125 other than that used to train the ANNs, was sourced for the southern coastline of  
126 Victoria. This data set had 222 presences but no absences were available. A schematic  
127 of the way in which these data sets were combined is presented in Figure 2.

128

### 129 **Data Preparation**

130

131 We used ArcGIS v9.2 to calculate the slope ( $^{\circ}$ ) and curvature (unit-less) of the seabed  
132 from the bathymetric data. We excluded areas known to be on-land, although a two-  
133 cell (i.e. 500 m) landwards buffer was included. This was because the spatial  
134 resolution of the bathymetric data was such that strictly following the shoreline as a  
135 cut-off would have excluded known inshore reefs. Seabed areas that were deeper than  
136 30 m, were also excluded, as there were no reef samples taken from deeper than 30 m.

137

138 A sliding window method was used to extract the slope data of grid cells surrounding  
139 each cell of the bathymetric grid, thus defining the input vectors for the artificial  
140 neural network (ANN). The sliding window conversion involved moving a sliding  
141 window of the specified size over the source matrix, as shown by the hypothetical  
142 example illustrated in Figure 3. Here, a three-by-three window starts centred on cell  
143 'g' (that is, the ANN will predict the presence of a reef in cell 'g'). The first vector  
144 produced is therefore composed of the contents of cells a, b, c, f, g, h, k, l and m. The

145 second vector is produced by sliding the window one cell to the right so that the  
146 window is centred on cell 'h' (that is, the ANN will predict the presence of a reef in  
147 cell 'h'). This vector is therefore composed of the contents of cells b, c, d, g, h, i, l, m  
148 and n. As this method only predicts for the centre cell of the window, the cells on the  
149 periphery of the matrix (a, b, c, d, e, f, j, k, o, p, t, u, v, w, x and y) do not have  
150 corresponding predictions of reef presence.

151

152 A window was not included in the final data set if it contained any missing data, that  
153 is, if part or the entire window were on land. The purpose of this process was to  
154 provide the context of the target cell (the middle of the sliding window) to the ANN.  
155 That is, rather than classifying from the value of the target cell, the classification  
156 decision was made from the cell and its context. The central assumption in this work  
157 is that reefs exist in similar contexts in the seabed, that is, the area of seabed  
158 surrounding a reef has similar characteristics to the area surrounding other reefs. We  
159 utilised a window size of 5 x 5 matrix elements to ensure that sufficient  
160 geomorphological context was presented to the ANN. There were 8 004 860 vectors  
161 extracted for this window.

162

163 We assigned output values to the vectors according to whether the target cell  
164 contained a point known to be either a reef or not a reef. Vectors that did not have a  
165 corresponding reef sample point (that is, where it was not known from survey data  
166 whether or not there was a reef in the corresponding target cell) were not included in  
167 the ANN training sets, but were retained for later use to generate the final map as  
168 described below in the subsection "ANN Model Application".

169



170 Bathymetric and curvature data were linearly rescaled according to the following  
171 formula:

172

$$173 \quad x_n = \frac{x - x_{min}}{x_{max} - x_{min}}$$

174

175 where  $x_n$  is the rescaled value of  $x$ ,  $x_{max}$  is the maximum value of variable  $x$ , and  
176  $x_{min}$  is the minimum value of  $x$ . The rescaling used the maximum and minimum  
177 possible values for these variables: for example, a depth of zero is the absolute  
178 minimum possible for bathymetric data, while the maximum was the 30 m cut-off  
179 depth used in the seabed data processing. The slope data was not linearly rescaled,  
180 because values were either zero or greater than 89. This data was rescaled by the  
181 simple process of subtracting 89 from any value that was not zero.

182

### 183 **ANN Algorithms**

184

185 The ANNs we used were three-neuron layer multi-layer perceptrons (MLP). These  
186 networks consisted of an input neuron layer, a single hidden neuron layer, and an  
187 output neuron layer. Each neuron layer was fully connected, that is, every neuron in a  
188 layer was connected to every neuron in the preceding neuron layer. The training  
189 algorithm used was unmodified backpropagation of errors with momentum  
190 (Rumelhart et al., 1986). This algorithm has been widely used in applications in  
191 ecology (Brosse et al., 2007; Brosse et al., 1999b; Bryant and Shreeve, 2002; Cocu et  
192 al., 2005; Dedecker et al., 2004; Dimopoulos et al., 1999; Fedor et al., 2008; Franci,  
193 2004; Gutiérrez-Estrada and Bilton, 2010; Joy and Death, 2002, 2004; Paul and  
194 Munkvold, 2005) and elsewhere (Bourland and Wellekens, 1987; Chandonia and

195 Karplus, 1995; Diederichs et al., 1998; Franzini, 1988; Haskey and Datta, 1998;  
196 Lippmann, 1989; Qian and Sejnowski, 1988; Rost, 1996) and is in many ways the *de*  
197 *facto* standard for training MLP. An advantage of MLP is that their outputs can be  
198 interpreted as probabilities (Kasabov, 1996).

199

## 200 **ANN Training and Evaluation**

201

202 We used ten-fold cross-validation to select the topology and training parameters of the  
203 MLP. That is, the training data set was randomly divided into ten equally sized  
204 subsets. One testing subset was held out and a MLP with randomly initialised  
205 connection weights trained over the remaining nine (the training fold). The trained  
206 MLP was recalled and its accuracy assessed over the training fold (giving the training  
207 accuracy) and the held-out testing set (the testing accuracy). The process was repeated  
208 ten times, with a different subset held out as the testing set each time. This gave an  
209 estimate of the generalisation accuracy of the MLP over the entire data set, and is not  
210 only widely recommended in the ANN literature (Flexer, 1996; Prechelt, 1996;  
211 Zhang, 2007) but has also been previously applied to ecological applications of ANN  
212 (Joy and Death, 2002, 2004).

213

214 The combinations of input variables we investigated were: slope of all cells in the  
215 window and bathymetric value of the target cell; curvature of all cells in the window  
216 and bathymetric value of the target cell; bathymetric values of the target cell with  
217 curvature and slope values of all cells in the window; bathymetric values of all cells in  
218 the window with curvature and slope of all cells in the window.

219

220 We investigated a number of different MLP topologies (number of hidden-layer  
221 neurons) and training parameters (learning rate, momentum, and training epochs)  
222 which were selected heuristically using expert knowledge. The mean generalisation  
223 accuracy (that is, the accuracy over the cross-validation testing subsets that the MLP  
224 were not trained on) of the MLP was used to select the combination of input variables  
225 and MLP parameters that gave the best accuracy.

226

227 Accuracy was measured firstly using Cohen's Kappa statistic (Cohen, 1960). A kappa  
228 of less than 0.2 is considered poor accuracy, 0.2 to 0.4 fair, 0.4 to 0.6 moderate, 0.6 to  
229 0.8 good and over 0.8 very good, with 1 being perfect accuracy. Kappa was used  
230 because it is a simple and well-known statistic (Manel et al., 2001) that is not biased  
231 by different proportions of presences or absences, and gives results that are  
232 qualitatively similar to more complex measures such as area under the receiver  
233 operating characteristic curve (Elith et al., 2006; Graham et al., 2008). The formula  
234 for kappa is:

$$\kappa = \frac{\Pr(a) - \Pr(e)}{1 - \Pr(e)}$$

235 where  $\kappa$  is the Kappa statistic,  $\Pr(a)$  is the observed agreement between the predicted  
236 and actual data, and  $\Pr(e)$  is the probability of chance agreement between the  
237 predicted and actual data.

238

239 The second accuracy measure used was percentages of data sets correctly classified.  
240 The first percentage measured was the percentage of examples out of each data set  
241 that were correctly classified, which while easily interpreted can also be biased by  
242 uneven proportions of classes in the data set, that is, an uneven number of presence  
243 and absence examples. To address this, the true positive and true negative percentage

244 accuracies were also measured. The true positive percentage is the percentage of  
245 positive examples that are correctly classified as positive, while the true negative  
246 percentage is the percentage of negative examples that are correctly classified as  
247 negative. While the final output of the MLP was the probability of each cell  
248 containing a reef, a threshold value of 0.5 was applied when calculating accuracies.  
249 That is, an output below 0.5 was considered to be negative, while an output above 0.5  
250 was considered to be positive. This threshold is reasonable given the interpretation of  
251 MLP outputs as probabilities. Also, the MLP output values for this problem (results  
252 not shown) consistently followed a U-shaped distribution, with most outputs close to  
253 either zero or unity.

254

255 The training parameters that yielded the best accuracies are presented in Table 1. In  
256 this work, the ‘best accuracies’ means that the networks had the best balance between  
257 learning the training data and being able to generalise to unseen data.

258

### 259 **ANN Model Application**

260

261 The parameters that gave the best cross-validated results were used to train MLP over  
262 the entire training set. As the random initialisation of connection weights in MLP can  
263 cause variations in the final accuracy of the trained networks, 100 MLP were trained.  
264 Accuracies were assessed over both the training data set (training accuracy) and the  
265 independent validation data set (giving the validation accuracy), that was sourced  
266 from a different survey as the training set. The final predictions of reef presence over  
267 the entire study region were generated using the MLP that had the highest accuracy  
268 over the validation data set (that is, that generalised the best). This gave the

269 probability that each cell contained a reef. As the validation data set was not used to  
270 select the topology or training parameters of the MLP, it remained independent. The  
271 process of selecting the optimal training parameters via ten-fold cross-validation, then  
272 further training over the complete training set and selecting the optimal MLP by  
273 validation error, is presented schematically in Figure 4.

274

### 275 ANN Contribution Analysis 276

277 Contribution analysis is a way of determining the relative importance of each input  
278 variable of the MLP with respect to the output. The method of contribution analysis  
279 used here was that of Olden and Jackson, (2002) which has been previously shown to  
280 be less biased in its assessment than other methods (Olden et al., 2004). This method  
281 yields unit-less values that show the relative positive or negative contribution of an  
282 input, where a positively contributing variable increases the activation of the output as  
283 the input variable increases and a negatively contributing variable decreases the  
284 activation as the variable increases. In the context of this application, a high value of a  
285 positively contributing variable is interpreted to be associated with the presence of a  
286 reef, while a high value of a negatively contributing variable is associated with the  
287 absence of a reef.

## 288 **Results** 289

290 The parameters that yielded the best mean cross-validated accuracies are presented in  
291 Table 1. These parameters yielded MLP that had the highest mean accuracies over the  
292 testing data sets, that is, they produced MLP that generalised to new data the best. The  
293 accuracies of the corresponding MLP are presented in Table 2. The input variables

294 that produced the highest test accuracies were the bathymetric value of the target cell,  
295 a 5 x 5 window of seafloor curvature and a 5 x 5 window of seafloor slope. For each  
296 combination of input variables, the cross-validated training accuracies were  
297 significantly higher (two-tailed  $t$ -test,  $p=0.001$ ) than the cross-validated testing  
298 accuracies. This implies that all networks over-trained to some extent; although the  
299 over-training was not severe in any case as the mean test kappas were all moderate to  
300 good. The true-positive and true negative percentage accuracies were similar,  
301 however, for both training and testing across all input data sets, which indicates that  
302 the cross validation data set was not badly unbalanced.

303

304 The parameters that produced the best cross-validated results were used to train MLP  
305 over the entire training set for each combination of variables. There were no  
306 significant differences between the cross-validated training accuracies and the  
307 accuracies over the complete training sets (two-tailed  $t$ -test,  $p=0.001$ ). The trained  
308 networks were assessed over the South Australian validation data set. The  
309 performance for all networks over the validation data set were poor, and in all cases  
310 the true positive percentage was low, indicating that the networks found it difficult to  
311 identify reefs in the South Australian validation data set. The exception to this was  
312 those trained with the bathymetric value of the target cell and a 5 x 5 window of  
313 slope, which was able to detect more than half of the reefs present. The best of these  
314 networks gave the validation accuracies presented in Table 4, which is a good kappa  
315 score and true positive detection rate of over 68%, with an overall accuracy of  
316 85.99%. As this network had the highest validation accuracy, that is, it classified  
317 unseen data the most accurately, it was used to create the final prediction map. The  
318 map generated by this MLP is displayed in Figure 5. Assessing this network over the

319 Victorian validation set gave a prediction accuracy of 52.25%, that is, the network  
320 correctly classified 52.25% of the reef cells.

321

322 The results of the MLP input contribution analysis of this network are presented in  
323 Figure 6. This shows that a high value of slope in the cells neighbouring the target cell  
324 contribute strongly to a prediction of a reef being present, and that a high bathymetric  
325 value contributes strongly to a prediction of a reef being absent.

326

## 327 **Discussion**

328

329 The need for a cost-effective standard method to map reefs across broad scales is  
330 likely to become an issue of increasing urgency as the world's coasts continue to bear  
331 the burden of the ecological costs of increasing human activity. South Australia  
332 presented one such locality in which this study sought to provide leadership in raising  
333 the challenges and solutions to what to date has been an intractable problem. In doing  
334 so we show that ANN provide a cost effective method for broadly mapping the  
335 probability of reef occurrence as a function of bathymetric and slope variables.

336

337 There were significant differences between the cross-validated training and testing  
338 accuracies for all combinations of input variables investigated; however the mean  
339 testing kappa scores were all moderate to good, which shows that the ANN did not  
340 badly over-train. The similarity between the true negative and true positive accuracies  
341 for both training and testing indicate that the cross-validation data set was not badly  
342 unbalanced in terms of positive and negative examples. There were no significant  
343 differences between the cross-validated training accuracies and the training accuracies

344 over the complete data set. This was expected, as the purpose of cross-validated  
345 training was to approximate the optimal training parameters. The poor performance  
346 over the South Australian validation data was the result of under-prediction of reef  
347 presences by the networks. Although the networks trained on bathymetric value, slope  
348 and curvature had the highest accuracies over the cross-validated testing sets, they  
349 exhibited poor performance at detecting reefs in the validation set. Conversely, the  
350 networks trained on bathymetric value and slope, while scoring the lowest accuracies  
351 over the cross-validated testing accuracies, achieved the highest accuracies over the  
352 validation data set.

353

354 It is likely that over-training was a major contributing factor to the under-prediction of  
355 reefs from the networks trained on a combination of bathymetric value, slope and  
356 curvature. It is well-known that a larger number of input features makes over-training  
357 of ANN more likely (Kasabov, 1996). This reinforces the importance of using an  
358 independent validation data set to verify the performance of any classifier, but  
359 especially so for data-driven models such as ANN.

360

361 Model performance over the spatially disparate Victorian validation set was lower  
362 (52.25% accuracy), indicating that a level of caution should be shown when using the  
363 MLP to extrapolate outside the region for which it was not trained. This is also likely  
364 to be a contributing reason that the performance over the South Australian validation  
365 set was slightly lower, as the points for this set also came from a slightly different  
366 area to the cross-validation training set. Validation using data sets that fall outside the  
367 area from which the model was trained are a stringent test of model performance,  
368 often resulting in a reduction in model performance (Barry and Elith, 2006).



369 However, it is possible that the lower performance index for Victoria could be the  
370 result of a difference in the geological context of reefs in South Australian compared  
371 to Victorian waters. To overcome problems with extrapolating outside the model  
372 region, future work should concentrate on the construction of region-specific  
373 classifiers wherever possible to account for this.

374

375 The results of the input contribution analysis show that the most important variables  
376 for the detection of reefs were the slope of the cells next to the target cell. A high  
377 slope value next to the target cell indicates the presence of a reef, while a high slope  
378 value in the target cell itself indicates the absence of a reef. This is reasonable, as a  
379 reef is likely to have a greater slope on its side than on its top. A high value of the  
380 bathymetric variable for the target cell indicated the absence of a reef, while a low  
381 value indicated reef presence. This also is reasonable, as a reef is an outcropping from  
382 the sea floor: reefs can therefore be expected to have a low bathymetric value, that is,  
383 they will not be as deep as cells without reefs. Of course, bathymetric depth alone is  
384 not enough to identify reefs, because of the range of depths at which reefs occur.

385

386 Although ANN were able to predict the location of reefs from bathymetric data (at  
387 least at depths less than 30 m) and measures of the slope of the seafloor, as data-  
388 driven methods, ANN are strongly affected by the quality of the data. There are two  
389 issues with the method used to prepare the data. The first is that the windowing  
390 technique excludes cells around the edges of the matrix, with the number of cells  
391 excluded being equal to half the window size. It also excludes cells that are less than  
392 half the window size from any area of no data, such as those that are close to areas  
393 deeper than 30 m, including those near to the continental shelf. Thus, a window size

394 of five will miss any reef within 500 m of the continental shelf. The second issue is  
395 that the resolution of the bathymetric data was 250 m. Therefore, this will miss any  
396 reefs smaller than 250 m. The coarse resolution of the data also caused problems with  
397 the placement of reef sample points. Some grid squares had two reef samples located  
398 within them. While for some grid squares this was the same reef, for others they were  
399 different reefs. Other grid squares had reefs in the same grid square as the coastline.  
400 Such data issues will cause problems for any classification algorithm (Kasabov,  
401 1996).

402

403 Our future work will focus on improving the accuracy of the predictions. One way of  
404 doing this would be to use ensembles of ANNs (Sharkey, 1996), which is where the  
405 predictions of several ANNs are combined to make one final prediction. In this  
406 approach, the individual ANN would be trained over particular geographic areas, and  
407 would thus be highly specialised. This has been shown to yield superior accuracies in  
408 other applications (Sharkey and Sharkey, 1997). While this would imply that the  
409 individual ANN were over-fitted to their target region, such diversity among members  
410 has been shown to be beneficial to ensembles (Brown, 2004; Minku et al., 2010). We  
411 will also investigate identifying specific types of reefs (steep, flat, etc.) based on  
412 structure and form. Whereas the work reported in this paper focussed on detecting  
413 reefs in general, the morphologies of different reef types may be different enough that  
414 specialising ANN on reef types may lead to better predictions overall. We will also  
415 investigate other ANN training algorithms, such as Levenberg-Marquardt (Masters,  
416 1995), resilient backpropagation (Riedmiller and Braun, 1993), and evolutionary  
417 programming (Fogel et al., 1997). Finally, there are several methods of variable  
418 selection (Abarbanel, 1993; Fernando et al., 2009; Gutiérrez-Estrada and Bilton,

419 2010; Sharma, 2000) that can be applied to the data set before constructing the ANN,  
420 which may yield improved ANN performance by reducing the number of variables to  
421 be modelled. The prevalence of reefs and unbalanced data sets is such that problems  
422 are likely to arise in modelling (Mouton et al., 2010). Bootstrapped training may help  
423 mitigate the effects of low prevalence and unbalanced training sets. Setting output  
424 thresholds using Bayesian statistics (Tarassenko, 1998) is also a possibility.

425

426 In conclusion, we have demonstrated a novel, but simple tool that may be used to  
427 uncover the location and extent of subtidal reefs and rocky habitats. While side-scan  
428 sonar is often used to establish fine scale information of habitat types, much of the  
429 world's reefs are yet to be identified at spatial extents that are sufficiently useful for  
430 ecologists and natural resource managers. This lack of fundamental information  
431 represents a critical gap in knowledge for basic predictions about the ubiquity of  
432 subtidal ecosystems and their contribution to the world's coastal ecology and  
433 economy. The knowledge gap persists because large parts of the world's coasts are  
434 inaccessible to traditional methods of mapping; i.e. SCUBA diving in seas of low  
435 visibility or high exposure to physical injury by the elements and wildlife and acoustic  
436 mapping is expensive and time consuming. Consequently, the methods developed  
437 here removes one of the largest obstacles to allowing marine biologists and resource  
438 managers to uncover the location and extent of some of the most diverse and  
439 productive marine ecosystems of the globe.

440

## 441 **Acknowledgements**

442 We thank J. Tanner for kindly supplying data for the non-reef habitat used to  
443 parameterise the model. The research was funded by Australian Research Council  
444 grants awarded to D.A. Fordham and S.D. Connell.

445 **References**

446

447 Abarbanel, H.D.I., 1993. The analysis of observed chaotic data in physical systems.  
448 *Reviews of Modern Physics* 65, 1331-1392.

449 Barry, S.C., Elith, J., 2006. Error and uncertainty in habitat models. *Journal of*  
450 *Applied Ecology* 43, 413-423.

451 Bourland, H., Wellekens, C.J., 1987. Multilayer Perceptrons and automatic speech  
452 recognition, IEEE First Annual Conference on Neural Networks, pp. 407-416.

453 Brosse, S., Grossman, G.D., Lek, S., 2007. Fish assemblage patterns in the littoral  
454 zone of a European reservoir. *Freshwater Biology* 52, 448-458.

455 Brosse, S., Guegan, J.-F., Tourenq, J.-N., Lek, S., 1999a. The use of artificial neural  
456 networks to assess fish abundance and spatial occupancy in the littoral zone of a  
457 mesotrophic lake. *Ecological Modelling* 120, 299-311.

458 Brosse, S., Guegan, J.F., Tourenq, J.N., Lek, S., 1999b. The use of artificial neural  
459 networks to assess fish abundance and spatial occupancy in the littoral zone of a  
460 mesotrophic lake. *Ecological Modelling* 120, 299-311.

461 Brown, G., 2004. Diversity in Neural Network Ensembles, School of Computer  
462 Science. University of Birmingham, Birmingham.

463 Bryant, S.R., Shreeve, T.G., 2002. The use of artificial neural networks in ecological  
464 analysis: estimating microhabitat temperature. *Ecological Entomology* 27, 424-432.

465 Chandonia, J.-M., Karplus, M., 1995. Neural Networks for Secondary Structure and  
466 Structural Class Predictions. *Protein Science* 4, 275-285.

467 Cochran, G.R., Lafferty, K.D., 2002. Use of acoustic classification of sidescan sonar  
468 data for mapping benthic habitat in the Northern Channel Islands, California.  
469 *Continental Shelf Research* 22, 683-690.

470 Cocu, N., Harrington, R., Rounsell, M.D.A., Worner, S.P., Hulle, M., 2005.

471 Geographical location, climate and land use influences on the phenology and numbers  
472 of the aphid, *Myzus persica*, in Europe. *Journal of Biogeography* 32, 615-632.

473 Cohen, J., 1960. A coefficient of agreement for nominal scales. *Educational and*  
474 *Psychological Measurement* 20, 37-46.

475 Connell, S.D., Gillanders, B.M., 2007. *Marine Ecology*. Oxford University Press,  
476 Melbourne 630 pp.

477 Crick, F., 1989. The recent excitement about neural networks. *Nature* 337, 129-132.

478 Dedecker, A.P., Goethals, P.L.M., Gariels, W., De Pauw, N., 2004. Optimization of  
479 Artificial Neural Network (ANN) model design for prediction of macroinvertebrates  
480 in the Zwlam river basin (Flanders, Belgium). *Ecological Modelling* 174, 161-173.

481 Diederichs, K., Freigang, J., Umhau, S., Zeth, K., Breed, J., 1998. Prediction by a  
482 neural network of outer membrane  $\beta$ -strand protein topology. *Protein Science* 7,  
483 2413-2420.

484 Dimopoulos, I., Chronopoulos, J., Chronopoulou, S., Lek, S., 1999. Neural network  
485 models to study the relationships between lead concentration in grasses and  
486 permanent urban descriptors in Athens city (Greece). *Ecological Modelling* 120, 157-  
487 165.

488 Elith, J., Graham, C.H., Anderson, R.P., Dudik, M., Ferrier, S., Guisan, A., Hijmans,  
489 R.J., Huettmann, F., Leathwick, J.R., Lehmann, A., Li, J., Lohmann, L.G., Loiselle,  
490 B.A., Manion, G., Moritz, C., Nakamura, M., Nakazawa, Y., Overton, J.M., Peterson,  
491 A.T., Phillips, S.J., Richardson, K., Scachetti-Pereira, R., Schapire, R.E., Soberon, J.,  
492 Williams, S., Wisz, M.S., Zimmermann, N.E., 2006. Novel methods improve  
493 prediction of species' distributions from occurrence data. *Ecography* 29, 129-151.

494 Fedor, P., Malenovsky, I., Vanhara, J., Sierka, W., Havel, J., 2008. Thrips  
495 (Thysanoptera) identification using artificial neural networks. Bulletin of  
496 Entomological Research 98, 437-447.

497 Fernando, T.M.K.G., Maier, H.R., Dandy, G.C., 2009. Selection of input variables for  
498 data driven models: An average shifted histogram partial mutual information  
499 estimator approach. Journal of Hydrology 367, 165-176.

500 Flexer, A., 1996. Statistical evaluation of neural network experiments: minimum  
501 requirements and current practice, 13th European Meeting on Cybernetics and  
502 Systems Research. Austrian Society for Cybernetic Studies, pp. 1005-1008.

503 Fogel, D.B., Wasson, E.C., Boughton, E.M., Porto, V.W., 1997. A step toward  
504 computer-assisted mammography using evolutionary programming and neural  
505 networks. Cancer Letters 119, 93-97.

506 Francl, L.J., 2004. Squeezing the turnip with artificial neural nets. Phytopathology 94,  
507 1007-1012.

508 Franzini, M.A., 1988. Learning to recognize spoken words: A study in connectionist  
509 speech recognition, in: Touretzky, D., Hinton, G., Sejnowski, T. (Eds.), Proceedings  
510 of the 1988 Connectionist Models Summer. Morgan Kaufmann, pp. 407-416.

511 Galparsoro, 2009. Predicting suitable habitat for the European lobster (*Homarus*  
512 *gammarus*), on the Basque continental shelf (Bay of Biscay), using Ecological-Niche  
513 Factor Analysis Ecological Modelling 220, 556-567.

514 Geoscience Australia, D.o.R., Energy and Tourism, Canberra, Australia, 2009.  
515 Australian Bathymetry and Topography Grid, GeoCat # 67703 ed. Australian  
516 Government, Geoscience Australia.

517 Graham, C.H., Elith, J., Hijmans, R.J., Guisan, A., Peterson, A.T., Loisele, B.A.,  
518 Group, T.N.P.S.D.W., 2008. The influence of spatial errors in species occurrence data  
519 used in distribution models. Journal of Applied Ecology 45, 239-247.

520 Guisan, A., Thuiller, W., 2002. Predicting species distribution: offering more than  
521 simple habitat models. Ecological Letters 8, 993-1009.

522 Gutiérrez-Estrada, J.C., Bilton, D.T., 2010. A heuristic approach to predicting water  
523 beetle diversity in temporary and fluctuating water. Ecological Modelling 221, 1451-  
524 1462.

525 Haskey, S.J., Datta, S., 1998. A Comparative Study of OCON and MLP Architectures  
526 for Phoneme Recognition, Proceedings of ICSLP 98.

527 Haykin, S., 1994. Neural networks: a comprehensive foundation. MacMillan  
528 Publishing Company.

529 Ibarra, A.A., Gevrey, M., Park, Y.-S., Lim, P., Lek, S., 2003. Modelling the factors  
530 that influence fish guilds composition using a back-propagation network: Assessment  
531 of metrics for indices of biotic integrity. Ecological Modelling 160, 281-290.

532 Jeong, K.-S., Kim, D.-K., Joo, G.-J., 2006. River phytoplankton prediction model by  
533 artificial neural network: Model performance and selection of input variables to  
534 predict time-series phytoplankton proliferations in a regulated river system.  
535 Ecological Informatics 1, 235-245.

536 Joy, M.K., Death, R.G., 2002. Predictive modelling of freshwater fish as a  
537 biomonitoring tool in New Zealand. Freshwater Biology 47, 2261-2275.

538 Joy, M.K., Death, R.G., 2004. Predictive modelling and spatial mapping of freshwater  
539 fish and decapod assemblages using GIS and neural networks. Freshwater Biology 49,  
540 1036-1052.

541 Kasabov, N.K., 1996. Foundations of Neural Networks, Fuzzy Systems, and  
542 Knowledge Engineering. MIT Press.

543 Laë, R., Lek, S., Moreau, J., 1999. Predicting fish yield of African lakes using neural  
544 networks. *Ecological Modelling* 120, 325-335.

545 Lek, S., Delacoste, M., Baran, P., Dimopoulos, I., Lauga, J., Aulagnier, S., 1996.  
546 Application of neural networks to modelling nonlinear relationships in ecology.  
547 *Ecological Modelling* 90, 39-52.

548 Lippmann, R.P., 1989. Review of Neural Networks for Speech Recognition. *Neural*  
549 *Computation* 1, 1-38.

550 Manel, S., Dias, J.-M., Ormerod, S.J., 1999. Comparing discriminant analysis, neural  
551 networks and logistic regression for predicting species distribution: a case study with  
552 a Himalayan river bird. *Ecological Modelling* 120, 337-347.

553 Manel, S., Williams, H.C., Ormerod, S.J., 2001. Evaluating presence-absence models  
554 in ecology: the need to account for prevalence. *Journal of Applied Ecology* 38, 921-  
555 931.

556 Marcos, M.S.A.C., Soriano, M.N., Saloma, C.A., 2005. Classification of coral reef  
557 images from underwater video using neural networks. *Optics Express* 13, 8766-9771.

558 Masters, T. (ed.) 1995. *Advanced Algorithms for Neural Networks, A C++*  
559 *Sourcebook*. Wiley, New York.

560 Mastrorillo, S., S., L., Dauba, F., Belaud, A., 1997. The use of artificial neural  
561 networks to predict the presence of small-bodied fish in a river. *Freshwater Biology*  
562 38, 237-246.

563 Mellin, C., Bradshaw, C.J.A., Meekan, M.G., Caley, M.J., 2010a. Environmental and  
564 spatial predictors of species richness and abundance in coral reef fishes. *Global*  
565 *Ecology and Biogeography* 19, 212-222.

566 Mellin, C., Russell, B.D., Connell, S.D., B.W., B., Fordham, D.A., 2010b.  
567 Geographic range determinants of two commercially important marine molluscs.  
568 submitted to *Diversity and Distributions*.

569 Minku, L.L., White, A.P., Yao, X., 2010. The Impact of Diversity on Online  
570 Ensemble Learning in the Presence of Concept Drift. *IEEE Transactions on*  
571 *Knowledge and Data Engineering* 22, 730-782.

572 Mouton, A.M., De Baets, B., Goethals, P.L.M., 2010. Ecological relevance of  
573 performance criteria for species distribution models. *Ecological Modelling* 221, 1995-  
574 2002.

575 Olden, J.D., Jackson, D.A., 2002. Illuminating the "black box": a randomization  
576 approach for understanding variable contributions in artificial neural networks.  
577 *Ecological Modelling* 154, 135-150.

578 Olden, J.D., Joy, M.K., Death, R.G., 2004. An accurate comparison of methods for  
579 quantifying variable importance in artificial neural networks using simulated data.  
580 *Ecological Modelling* 178, 389-397.

581 Paul, P.A., Munkvold, G.P., 2005. Regression and artificial neural network modeling  
582 for the prediction of gray leaf spot of maize. *Phytopathology* 95, 388-396.

583 Prechelt, L., 1996. A quantitative study of experimental evaluations of neural network  
584 learning algorithms: Current research practice. *Neural Networks* 9, 457-462.

585 Qian, N., Sejnowski, T.J., 1988. Predicting the Secondary Structure of Globular  
586 Proteins Using Neural Network Models. *Journal of Molecular Biology* 202, 865-884.

587 Reed, R.D., Marks, R.J., 1999. *Neural smithing*. MIT Press.

588 Riedmiller, M., Braun, H., 1993. A direct adaptive method for faster backpropagation  
589 learning: The RPROP algorithm, *IEEE International Conference on Neural Networks*.  
590 IEEE, San Francisco.

591 Robinson, L.M., Elith, J., Hobday, A.J., Pearson, R.G., Kendall, B.E., Possingham,  
592 H.P., Richardson, A.J., 2010. Pushing the limits in marine species distribution

593 modelling: lessons from the land present challenges and opportunities. *Global*  
594 *Ecology and Biogeography*.  
595 Rost, B., 1996. PHD: Predicting One-Dimensional Protein Structure by Profile-Based  
596 Neural Networks. *Methods in Enzymology* 266, 525-539.  
597 Rumelhart, D.E., Hinton, G.E., Williams, R.J., 1986. Learning representations by  
598 back-propagating errors. *Nature* 323, 533-536.  
599 Sharkey, A.J.C., 1996. On Combining Artificial Neural Nets. *Connection Sciences* 8,  
600 299-313.  
601 Sharkey, A.J.C., Sharkey, N.E., 1997. Combining diverse neural nets. *The Knowledge*  
602 *Engineering Review* 12, 231-247.  
603 Sharma, A., 2000. Seasonal to interannual rainfall probabilistic forecast for improved  
604 water supply management: Part 1 - A strategy for system predictor identification.  
605 *Journal of Hydrology* 239, 232-239.  
606 Soltic, S., Pang, S., Peacock, L., Worner, S., 2004. Evolving computation offers  
607 potential for estimation of pest establishment. *International Journal of Computers,*  
608 *Systems and Signals* 5, 36-43.  
609 Tarassenko, L., 1998. *A guide to neural computing applications*. Wiley, London.  
610 Wagner, R., Dapper, T., Schmidt, H.-H., 2000. The influence of environmental  
611 variables on the abundance of aquatic insects: a comparison of ordination and  
612 artificial neural networks. *Hydrobiologica* 422/423, 143-152.  
613 Wagner, R., Obach, M., Werner, H., Schmidt, H.-H., 2006. Artificial neural nets and  
614 abundance prediction of aquatic insects in small streams. *Ecological Informatics* 1,  
615 423-430.  
616 Zhang, G.P., 2007. Avoiding Pitfalls in Neural Network Research. *IEEE Transactions*  
617 *on Systems, Man and Cybernetics - Part C: Applications and Reviews* 37, 3-16.  
618 Zhou, X., Chen, Y., 2005. Seafloor Classification of Multibeam Sonar Data Using  
619 Neural Network Approach. *Marine Geodesy* 28, 201-220.  
620  
621

622

623

| Inputs              | Hidden Neurons | Epochs | Eta  | Alpha |
|---------------------|----------------|--------|------|-------|
| Bathy-1 Curva       | 16             | 14000  | 0.25 | 0.15  |
| Bathy-1 Curva Slope | 15             | 10000  | 0.3  | 0.1   |
| Bathy-1 Slope       | 17             | 15000  | 0.15 | 0.15  |
| Bathy Curva Slope   | 15             | 10000  | 0.3  | 0.1   |

624

625

626

627

628

629

**Table 1 – training parameters for best performing MLP. ‘Bathy’ is a window of bathymetric values; ‘Bathy-1’ is the bathymetric value of the target cell; ‘Curva’ is the curvature of the seabed; ‘Slope’ is the slope of the sea bed. ‘Eta’ is the backpropagation learning rate parameters. ‘Alpha’ is the backpropagation momentum parameter.**



630  
631

|                      | Bathy-1 Curva    | Bathy-1 Curva Slope | Bathy-1 Slope    | Bathy Curva Slope |
|----------------------|------------------|---------------------|------------------|-------------------|
| <b>Train K</b>       | <b>0.88±0.01</b> | <b>0.93±0.02</b>    | <b>0.77±0.04</b> | <b>0.90±0.07</b>  |
| Train overall %      | 94.70±0.52       | 96.65±0.89          | 89.10±1.83       | 95.49±2.97        |
| Train true pos. %    | 85.95±1.37       | 95.49±1.94          | 92.94±2.70       | 91.46±8.32        |
| Train true neg. %    | 99.89±0.23       | 97.34±0.92          | 86.84±2.84       | 97.82±0.83        |
| <b>Test K</b>        | <b>0.70±0.12</b> | <b>0.77±0.06</b>    | <b>0.51±0.13</b> | <b>0.71±0.09</b>  |
| Test overall %       | 86.77±6.16       | 89.54±2.91          | 76.91±5.48       | 87.37±3.46        |
| Test true pos. %     | 66.67±11.60      | 85.45±9.57          | 72.90±11.48      | 73.73±11.56       |
| Test true neg. %     | 99.00±2.11       | 93.47±6.18          | 79.08±7.70       | 95.84±3.27        |
| <b>Complete K</b>    | <b>0.87±0.03</b> | <b>0.91±0.04</b>    | <b>0.72±0.09</b> | <b>0.92±0.03</b>  |
| Complete overall %   | 94.03±1.46       | 95.76±1.69          | 82.3±14.03       | 96.32±1.58        |
| Complete true pos. % | 85.48±3.81       | 93.60±3.42          | 89.65±5.72       | 94.66±3.73        |
| Complete true neg. % | 99.10±2.97       | 97.04±2.19          | 86.9±3.55        | 97.31±1.74        |
| <b>Validate K</b>    | <b>0.0±0.0</b>   | <b>0.17±0.12</b>    | <b>0.46±0.10</b> | <b>0.0±0.02</b>   |
| Validate overall %   | 72.84±0.0        | 73.8±3.55           | 79.91±3.18       | 72.08±1.27        |
| Validate true pos. % | 0.0±0.0          | 19.59±9.70          | 53.25±10.50      | 2.17±1.17         |
| Validate true neg. % | 100.0±0.0        | 94.04±3.88          | 89.85±2.89       | 98.15±1.86        |

632 Table 2 – accuracies of MLP trained on 5 x 5 windows. Column labels describe the input variables of the  
633 networks: ‘Bathy’ is a window of bathymetric values; ‘Bathy-1’ is the bathymetric value of the target cell;  
634 ‘Curva’ is the curvature of the seabed. Rows labelled ‘Train’ are the accuracies over the training data sets.  
635 Rows labelled ‘Test’ are accuracies over the test sets, that is, the data sets that the MLP have not been  
636 trained on. Rows labelled ‘Complete’ are accuracies over the complete, combined training and testing set,  
637 that is, the training accuracies of the MLP over which the validation accuracies were assessed. Rows  
638 labelled ‘Validate’ are the accuracies over the independent validation data set. ‘K’ denotes Cohen’s kappa  
639 and ‘%’

640

641

642

---

|                 |       |
|-----------------|-------|
| Kappa           | 0.63  |
| Overall %       | 85.99 |
| True Positive % | 68.25 |
| True Negative % | 92.60 |

643

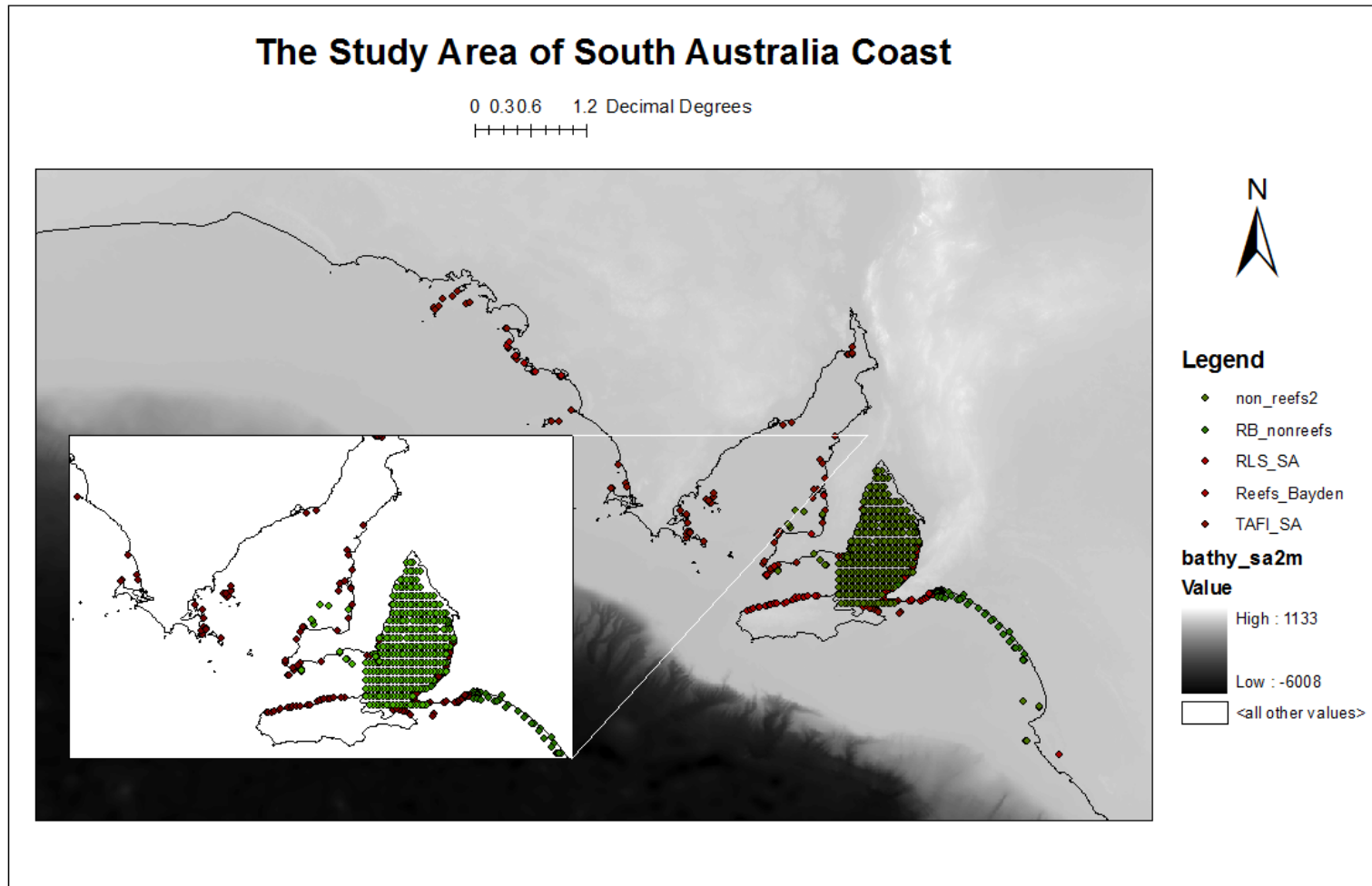
644

645

---

**Table 3 – accuracies over independent validation set of MLP used to generate final prediction maps. Row and column heading are as for Tables 2 and 3.**

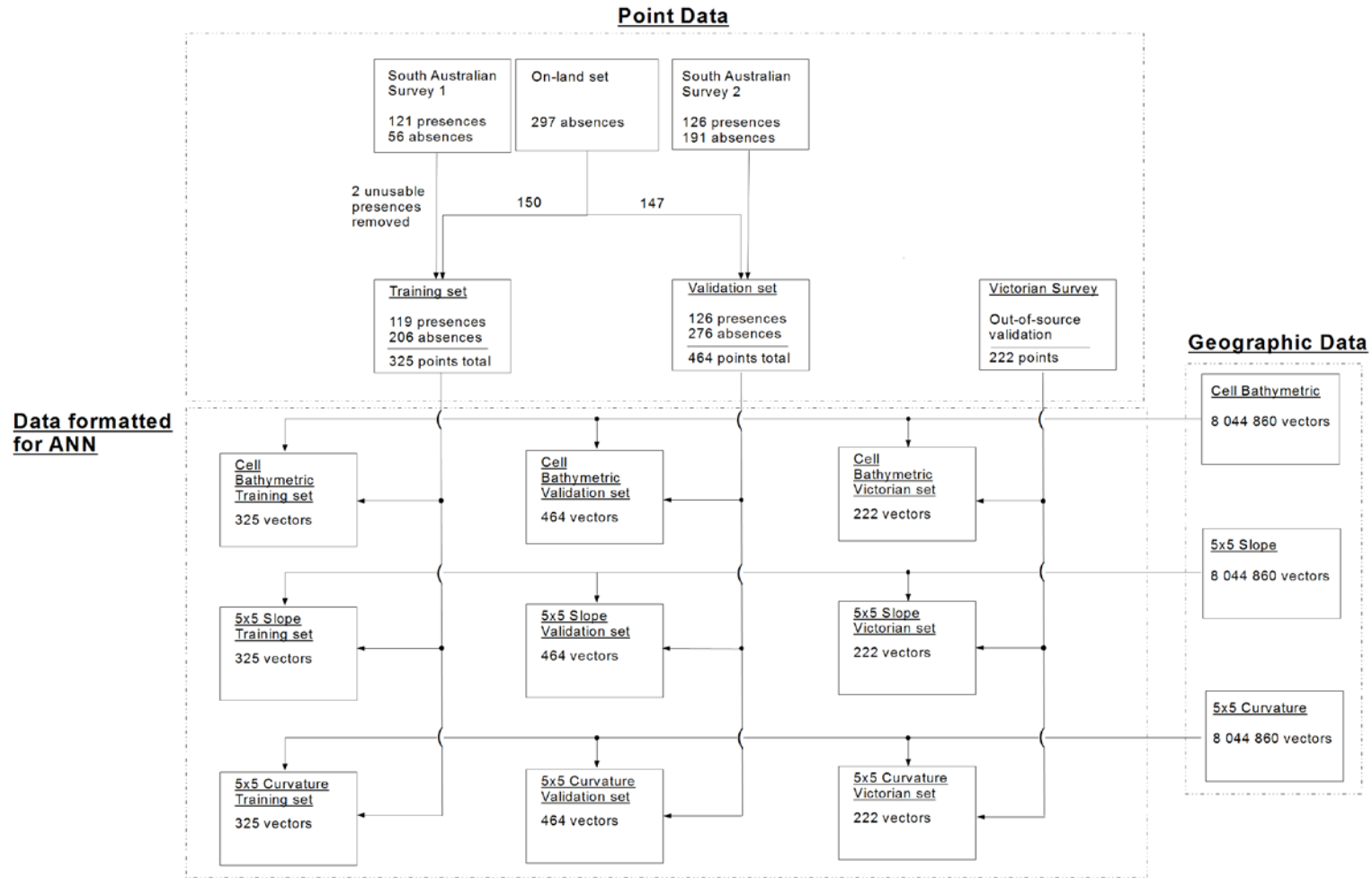
646



647  
648  
649

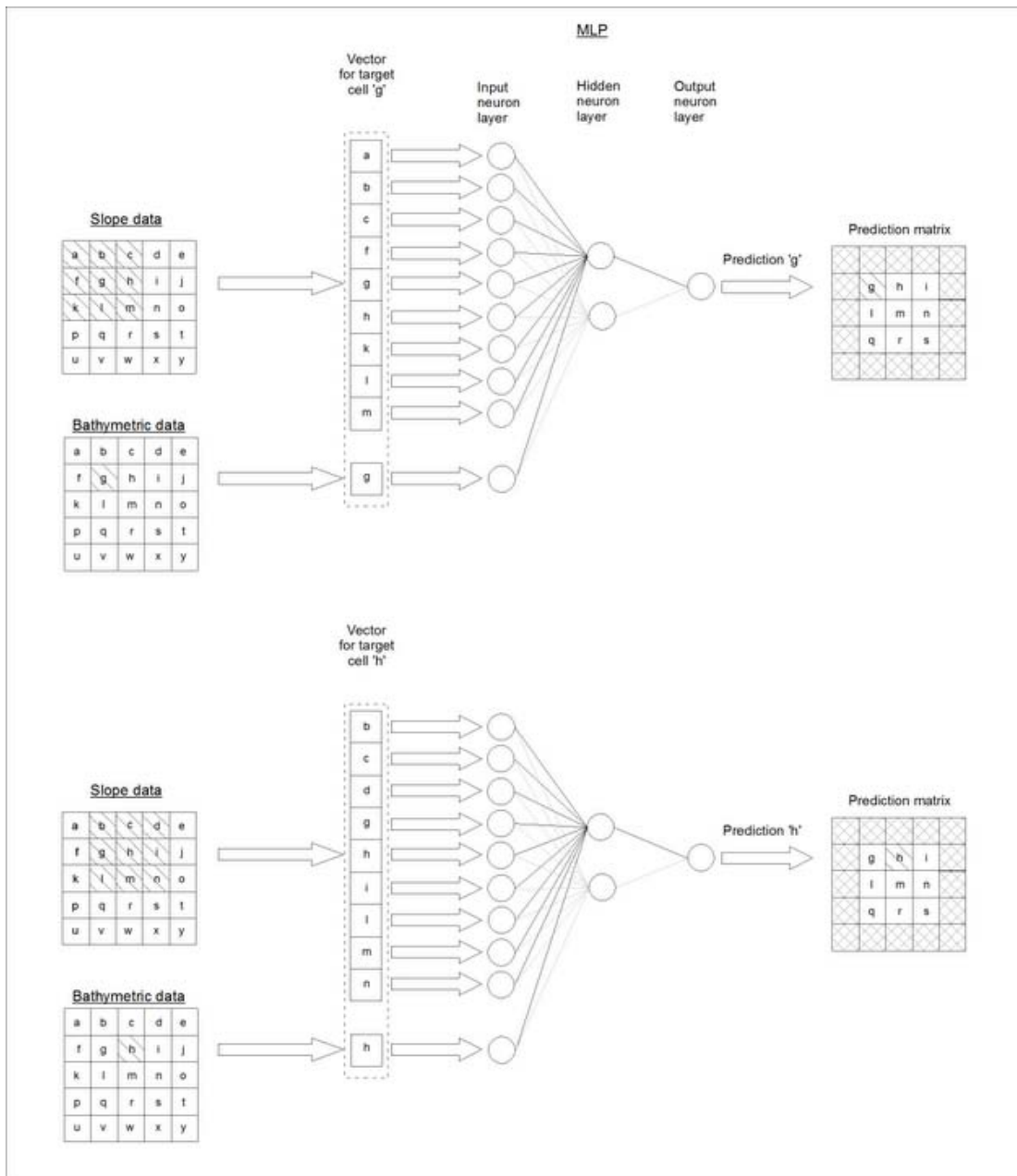
Figure 1 –map of the study area, the South Australian coastline and Kangaroo Island. The insert is a zoomed-in view of the central study area within the Spencer Gulf and the Gulf St Vincent. The study area goes from latitude -38 to -31 degrees, and longitude 129 to 141 degrees.

650



651

652 Figure 2 – combining source data sets to create ANN training data sets. The arrows show the flow of data from one set to another.

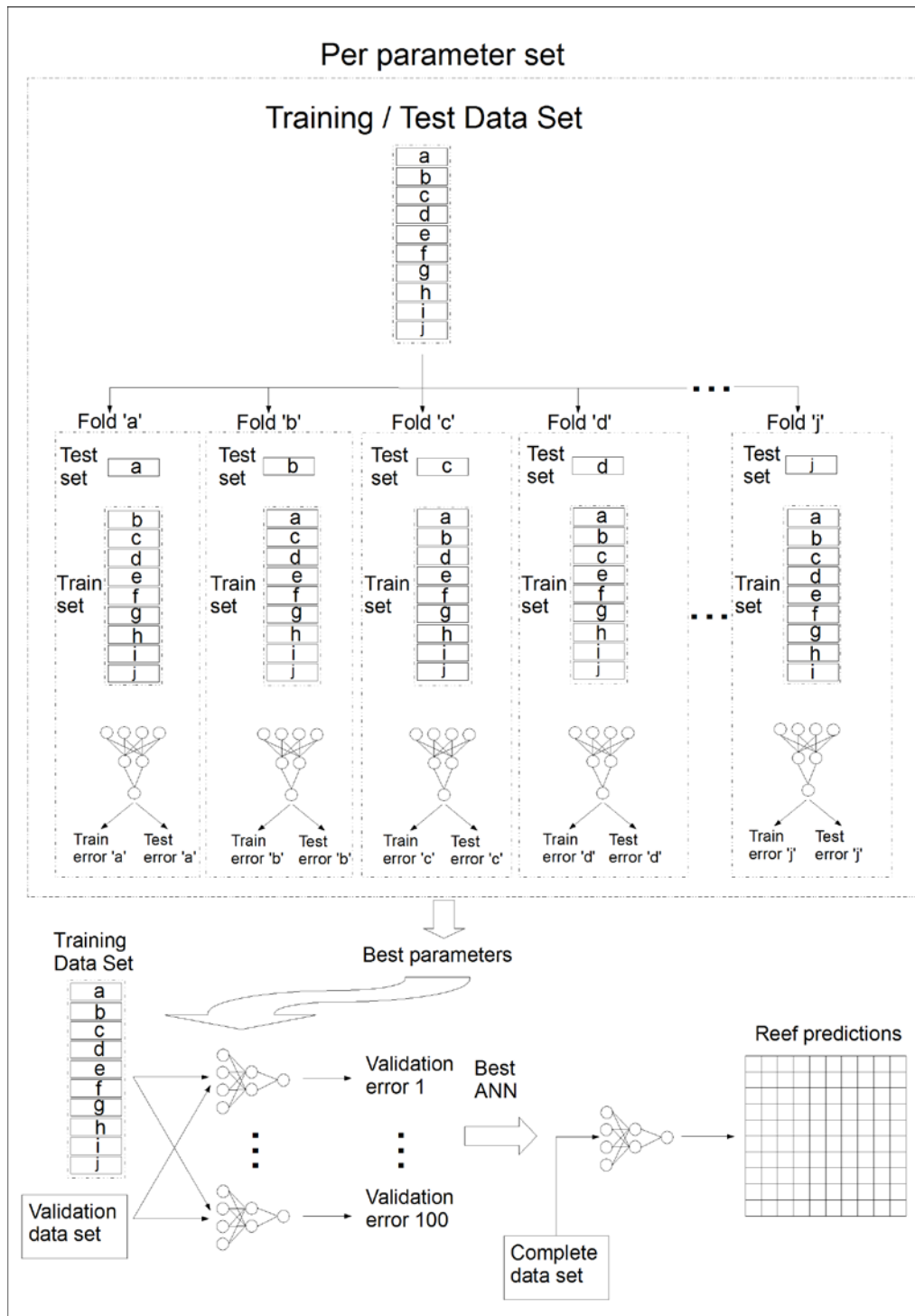


653

654 **Figure 3 - encoding and prediction process for a 3-by-3 window of slope data and a single cell for**  
 655 **bathymetric data. Two example vectors are being produced here. For the first, the target cell is cell 'g'. For**  
 656 **the second, the target cell is cell 'h'. The cross-hatching in the prediction matrix shows the cells that are**  
 657 **excluded from the predictions by the windowing process. Note that not all input neurons of the multi-layer**  
 658 **perceptron (MLP) are shown**

659

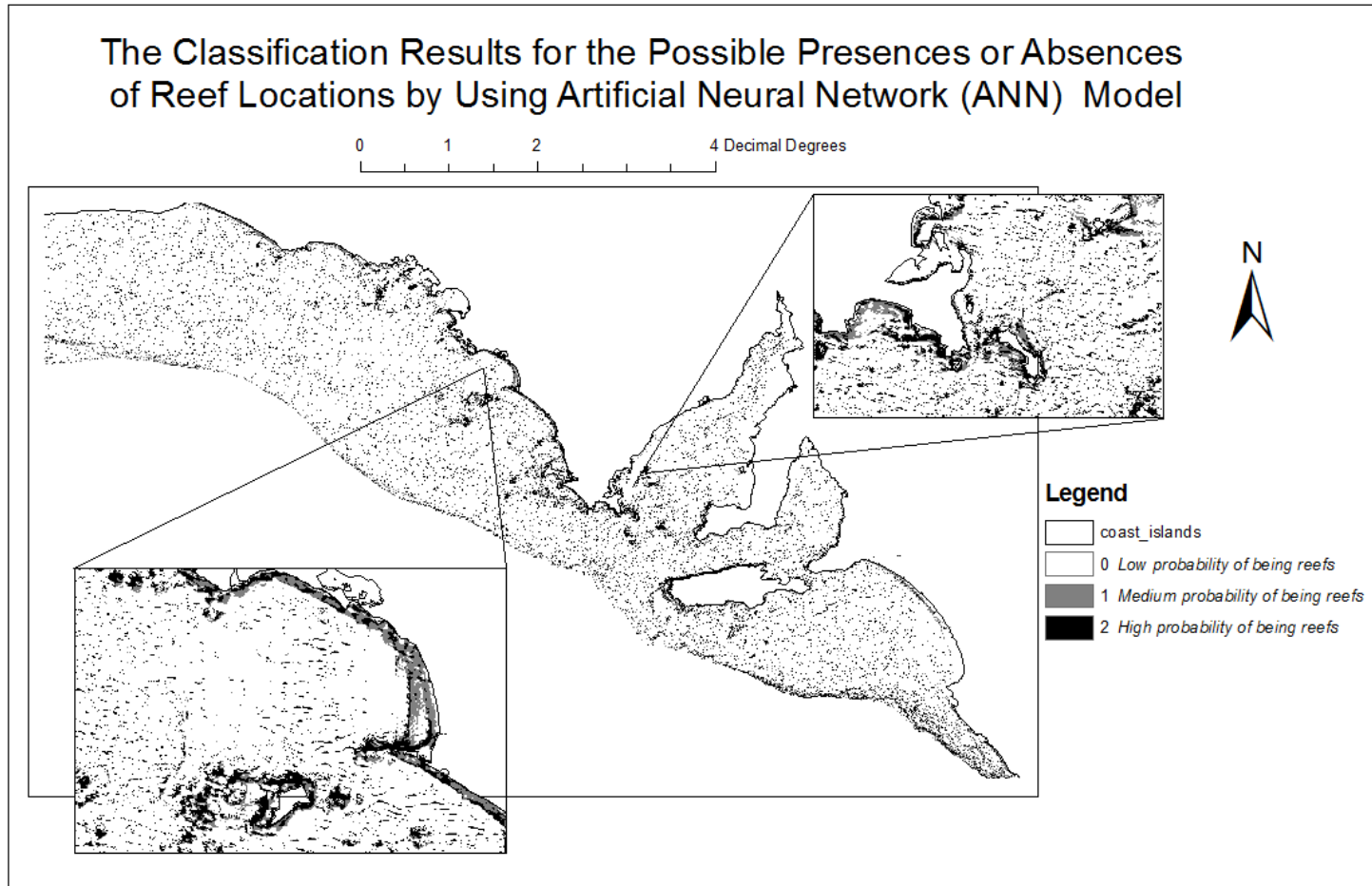
660



662  
 663  
 664  
 665

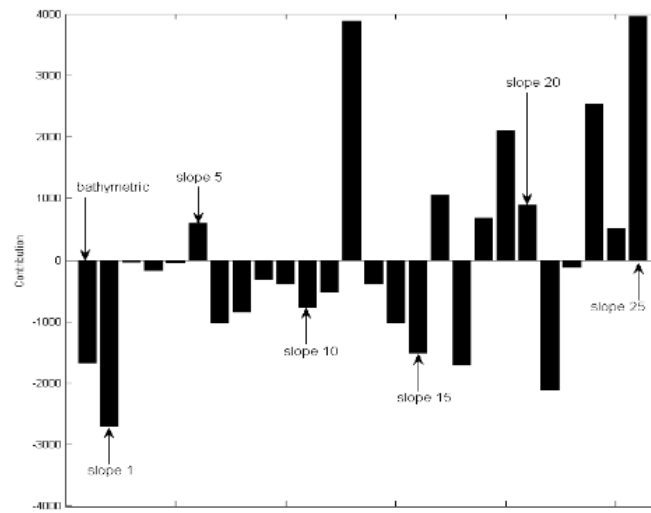
Figure 4 – schematic of cross-validation selection of training parameters, training over complete training set, selection of most accurate network and production of reef predictions.

666

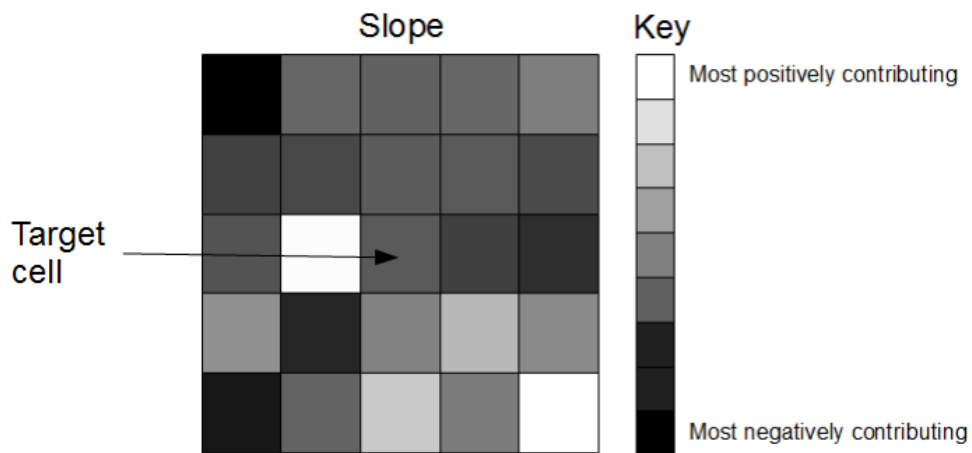


667

668 Figure 5 - Map of South Australian reefs generated by MLP trained on 5x5 input windows. Brighter colours are equal to higher probabilities of reef presences. Land masses are  
669 white and delimited by lines. The inserts are zoomed-in views of two areas on the South Australian coast and the Eyre peninsula. Areas deeper than 30 m have been masked out, as  
670 have areas on land.



(a) contributions by input variable



(b) slope contributions by grid cell

672

673 **Figure 6 - Results of MLP input contribution for bathymetric value of target cell and a 5x5 window of**  
 674 **seabed slope. In (a) the values of each variable are charted, with the variable corresponding to the**  
 675 **bathymetric and slope variables labelled. In (b) the contributions of the slope variables are gridded**  
 676 **according to their position in the sliding window and shaded according to their contribution, with the most**  
 677 **positive contributions being white and the most negative contributions black.**

678